

# Anisotropic Diffusion for Medical Image Enhancement

**Nezamoddin N. Kachouie**

nezam.nk@gmail.com

*Department of Systems Design Engineering,  
University of Waterloo, Waterloo, ON, Canada  
Present Affiliation: Harvard-MIT Health  
Sciences and Technology Harvard  
Medical School, Cambridge, MA, USA*

---

## Abstract

Advances in digital imaging techniques have made possible the acquisition of large volumes of Trans-rectal Ultrasound (TRUS) prostate images so that there is considerable demand for automated segmentation of these images. Prostate cancer diagnosis and treatment rely on segmentation of TRUS prostate images. This is a challenging and difficult task due to weak prostate boundaries, speckle noise, and narrow range of gray levels which leads most image segmentation methods to perform poorly. Although the enhancement of ultrasound images is difficult, prostate segmentation can be potentially improved by enhancement of the contrast of TRUS images. Anisotropic diffusion has been used for image analysis based on selective smoothness or enhancement of local features such as region boundaries. In its conventional form, anisotropic diffusion tends to encourage within-region smoothness and avoid diffusion across different regions. In this paper we extend the anisotropic diffusion to multiple directions such that segmentation methods can effectively be applied based on rich extracted features. A preliminary segmentation method based on extended diffusion is proposed. Finally an adaptive anisotropic diffusion is introduced based on image statistics.

**Keywords:** TRUS Imaging, Deformable Models, Level Sets, Anisotropic Diffusion, Segmentation.

---

## 1. INTRODUCTION

As the most diagnosed cancer, prostate cancer is the second leading cause of the cancer death in North America [1]. Hence diagnosis of this cancer in its early stages is crucial. Prostate TRUS images, in comparison with the other modalities such as CT and MRI, are captured more easily, in real-time, and with lower cost, so they are widely used for the diagnosis of prostate cancer, cancer treatment planning, needle biopsy, and brachytherapy. The size and the shape of the prostate must be determined by prostate segmentation to diagnose the cancer stage. Although in the traditional approach, an expert infers this information manually from the TRUS images, such a manual method is tedious, expensive, time consuming, and subjective. Given the increasing amount of TRUS data being collected, automated methods of TRUS prostate segmentation are in high demand and different segmentation methods have been proposed [2, 3, 4, 5, 6, 7, 8, 9]. These methods include boundary segmentation, deformable models, and region segmentation approaches.

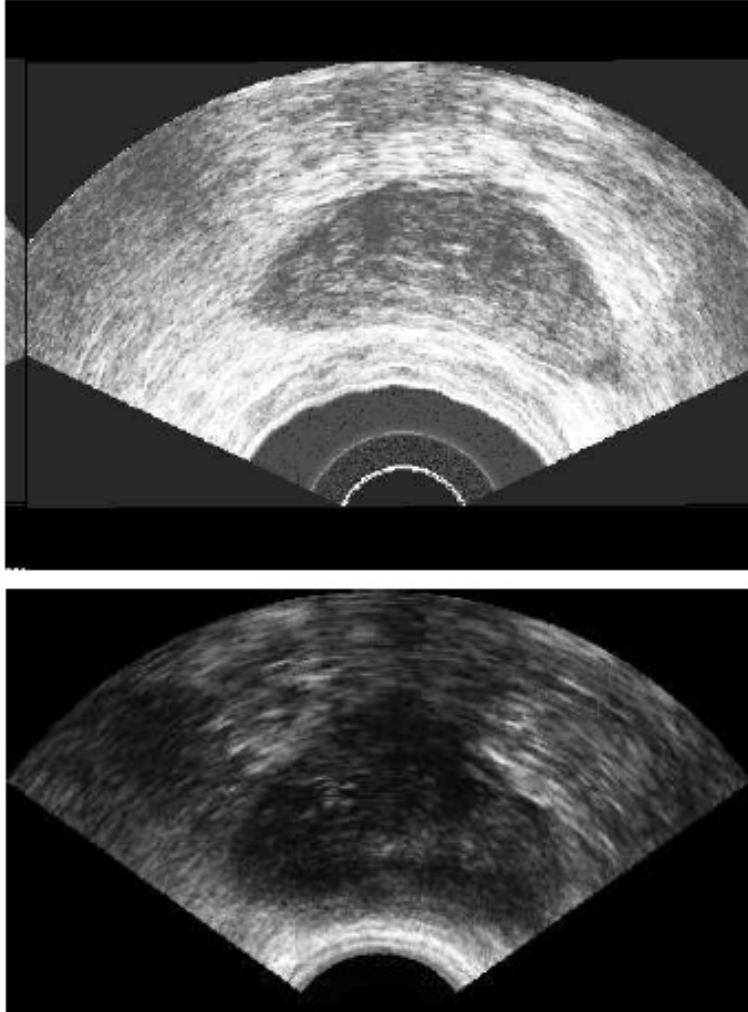


**FIGURE 1:** Two TRUS prostate images.

The prostate region in TRUS prostate images usually maintains a very weak contrast against the background. Because of the speckle noise, short range of gray levels, very weak prostate region texture, and shadow regions the conventional image processing and analysis techniques are not capable to effectively capture, discriminate, and segment the prostate region based on its intensity, texture, and gradient. There have been some attempts by employing the Gabor filter bank for prostate texture segmentation [10, 5], however prostate has a very weak texture and has not yet been investigated seriously.

Anisotropic diffusion [11] was introduced by Prona and Malik to perform edge preserving and within-region smoothing based on the differential structure of the image [12, 13]. Anisotropic diffusion considers no prior information about the regions and boundaries, and does selective diffusion based on local computation of a conduction term. Moreover, anisotropic diffusion computes group diffusion as a single diffusion value for each spatial location by summation of diffusions in four directions in each time step. There are some weak radial and angular features in ultrasound images which potentially can be used to reveal weak structures and textures. Our goal in this paper is extending anisotropic diffusion to multiple directions which are computed independently for contrast enhancement of TRUS images. Therefore, eight anisotropic diffusion values will be computed independently for each spatial location. This can provide a rich feature space with potential use in image analysis and segmentation.

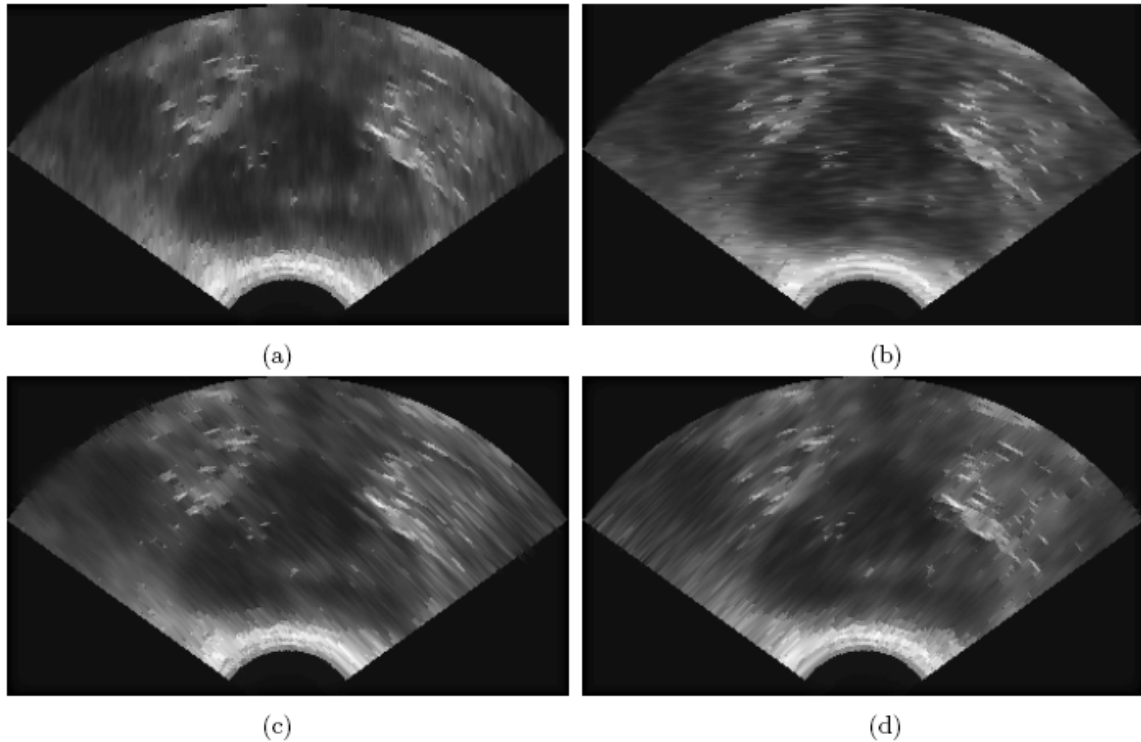


**FIGURE 2:** Application of extended anisotropic diffusion in eight directions. (a) North-South. (b) East-West. (c) NE-SW. (d) NW-SE.

Moreover, considering a semi-supervised segmentation such as deformable models to initialize a seed, we introduce an adaptive anisotropic diffusion in which the estimated statistics extracted from the region of interest can be used to adaptively switch between different conduction functions leading to better within-region smoothness while preserving the region boundaries.

## 2. The Proposed Method

Strong region boundaries are desired for image segmentation, however image denoising tends to smooth sharp boundaries of the image and reduces the image contrast. To overcome this drawback of image denoising methods, anisotropic diffusion method, as an alternative to linear-filtering was introduced by Perona and Malik [11]. Anisotropic diffusion considers a conduction term that is locally computed and depends on the differential structure of the image. Anisotropic diffusion filter was used by Gerig et al. [12] to enhance MR images. To perform edge preserving and within region smoothing of MR images, Sapiro and Tannenbaum [13] used a similar approach.

### Anisotropic Diffusion

Perona and Malik [11] presented the anisotropic diffusion filter as a diffusion process that encourages intra-region smoothness while inhibits inter-region smoothness. Mathematically, the process is defined as follows:

$$\frac{\partial}{\partial t} I(\bar{x}, t) = \nabla \cdot (c(\bar{x}, t) \nabla I(\bar{x}, t)) \quad (1)$$

where  $I(x,0)$  is the initial unprocessed image,  $x$  is the image coordinate and  $t$  is the iteration step.  $c(x,t)$  is the diffusion function and is a monotonically decreasing function of the image gradient magnitude. To encourage smoothing within a region and discourage it across different regions, the conduction coefficient  $c$  must be set to one inside the region (smooth conduction) and set to zero otherwise. For edge estimation to locate the region boundaries, the gradient of intensity image is first obtained:

$$\hat{E}(\bar{x}, t) = \nabla(I(\bar{x}, t)) \tag{2}$$

The conduction coefficient of diffusion is then computed locally as a gradient magnitude of local image intensities:

$$c(\bar{x}, t) = f(\|\nabla(\bar{x}, t)\|) \tag{3}$$

By the proper selection of function  $f$ , not only region boundaries can be preserved but also edges maybe sharpened. Any monotonically decreasing continuous function of  $\|\nabla I\|$  could be selected as a diffusion function. Two functions for local computation of the conduction to satisfy selective edge smoothness and enhancement were suggested by Perona and Malik [11]. The first one

$$c(\bar{x}, t) = \exp\left(-\left(\frac{\|\nabla(\bar{x}, t)\|}{\kappa}\right)^2\right) \tag{4}$$

encourages high contrast edges over low contrast ones while the second function

$$c(\bar{x}, t) = \frac{1}{1 + \left(\left(\frac{\|\nabla(\bar{x}, t)\|}{\kappa}\right)^2\right)} \tag{5}$$

encourages wide regions over smaller regions where  $k$  is the diffusion coefficient. The differential relation in (1) can be discretized and be numerically implemented as

$$I_{i,j}^{t+1} = I_{i,j}^t + \eta \left( N_c \cdot \nabla_N I + S_c \cdot \nabla_S I + W_c \cdot \nabla_W I + E_c \cdot \nabla_E I \right) \tag{6}$$

where  $N_c$ ,  $S_c$ ,  $W_c$ , and  $E_c$  are conduction in north, south, west, and east directions respectively and  $\square$  is the step size.

**Extended Diffusion**

We extended anisotropic diffusion to multiple directions to be used to reveal weak radial and angular features in ultrasound images. This rich feature set can be used for contrast enhancement, image analysis, and segmentation. We apply anisotropic diffusion in eight directions, generating four diffused images computed independently regarding four directional pairs for each spatial location. Thus the anisotropic diffusion is computed for North-South and East-West directions separately and is extended by introducing two new directions as North-East

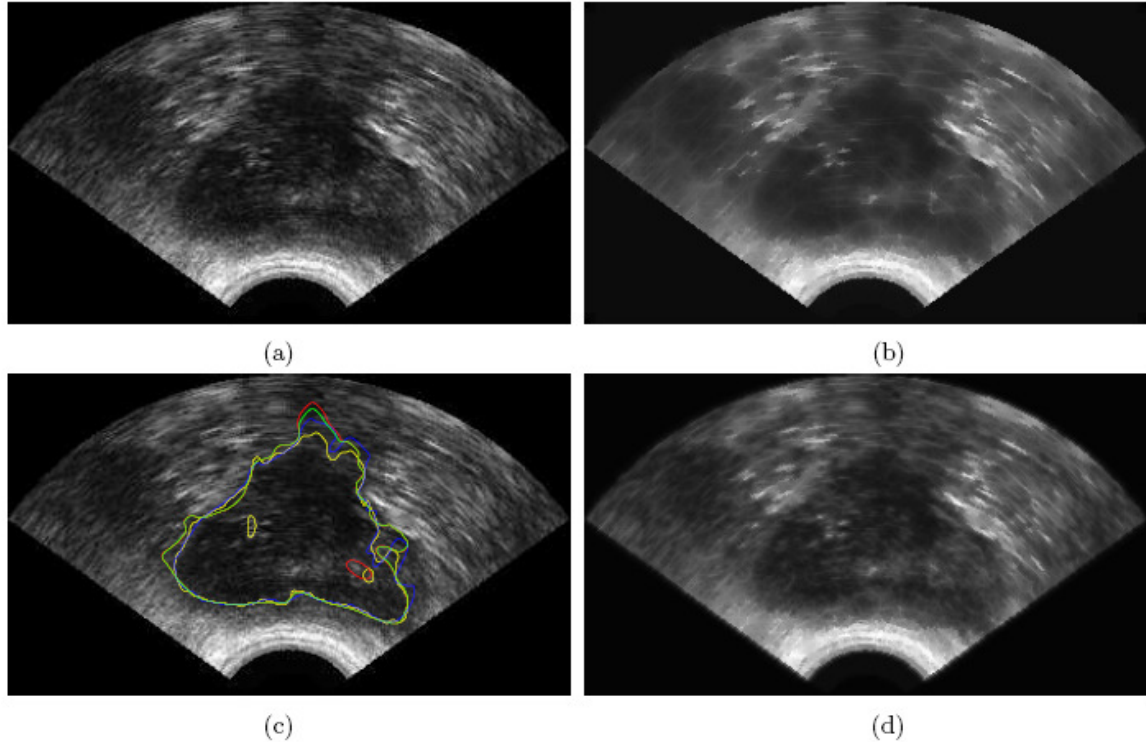


Figure 3: (a) Unprocessed TRUS image. (b) Extracted maximum diffusion over all diffused images. (c) Deformations of different contours over specific diffusion directions. (d) Application of adaptive anisotropic diffusion and extraction of maximum diffusion over all diffused images.

to South-West, i.e., 45 degree, and North-West to South-East, i.e., 135 degree. Recalling (1), considering the gradient in a specific single direction, diffusion can be simplified as

$$\nabla \cdot (c(\bar{x}, t) \nabla I_R(\bar{x}, t)) = \frac{\partial}{\partial R} (c(\bar{x}, t) I_R) \quad (7)$$

where  $R$  is any of four direction pairs, i.e., horizontal, vertical, 45 degree, and 135 degree. By definition,  $c(x, t) I_R$  is called flux in  $R$  direction,  $\Phi(I_R)$ . One dimensional diffusion can be decomposed to the four independent fluxes as:

$$\frac{\partial}{\partial R} (\Phi(I_R)) = \Phi'(I_R) \cdot I_{RR} \quad (8)$$

where  $c(x, t)$  is replaced with  $f(\|\nabla(\bar{x}, t)\|)$ .

### Adaptive Anisotropic Diffusion

Most often a semi-supervised method is used for region segmentation for example by initializing a seed or initiate a contour. We propose an adaptive anisotropic diffusion such that the estimated statistics which are extracted from the region of interest can be used to adaptively select the conduction function which potentially may lead to a better within-region smoothness while could preserve the region boundaries. Therefore, to encourage the smoothness and discourage the diffusion based on image statistics and image features more effectively, an adaptive conduction is introduced.

$$c(\bar{x}, t) = \exp\left(-\left(\frac{\|\nabla(\bar{x}, t)\|}{\kappa}\right)^2\right) \quad \forall \bar{x} \in G \quad (9)$$

otherwise,

$$c(\bar{x}, t) = C \quad \forall \bar{x} \notin G \quad (10)$$

where  $C$  is a constant conduction factor and  $G$  is some definition of the region, for example

$$\bar{x} \in G \text{ if } I_{\bar{x}}^t \in [\mu - \sigma, \mu + \sigma]$$

for some region mean and standard deviation. Diffusion is encouraged within the region based on constant conduction factor. However, outside the region, diffusion will follow the formal conduction function (4).

### Level Sets

A level set contour will be initialized and deformed toward prostate boundary. External force that controls the deformations of the zero level set toward the prostate boundary is extracted by applying the anisotropic diffusion in four directional diffusion pairs. To generate the external force for each spatial location of the TRUS image, the maximum diffusion among directional diffusions is selected.

Starting contour which is the zero level set of a 3D volume will be initialized by user interactions. It could also be initialized as an elliptical level set by selecting the ellipse centre. The statistics of the region of the interest are estimated over the initialized contour to be used for adaptive anisotropic diffusion. Having the zero level set initialized as an elliptical contour, velocity function  $F$  is designed based on the extracted features from diffused images so that the interface evolves toward the prostate boundary and converges in its vicinity.

$$F = -\exp\{\epsilon \kappa - \alpha \times D_v\} \quad (11)$$

where  $\kappa$  and  $\square$  are curvature and curvature coefficient respectively,  $D_v$  is velocity derived by external energy which is extracted from diffused images,  $\alpha$  is a velocity constant coefficient and

$$\kappa = \nabla \cdot \frac{\nabla \Phi}{|\nabla \Phi|} = \left\{ \frac{\Phi_{xx}\Phi_y^2 - 2\Phi_x\Phi_y\Phi_{xy} + \Phi_{yy}\Phi_x^2}{(\Phi_x^2 + \Phi_y^2)^{\frac{3}{2}}} \right\} \quad (12)$$

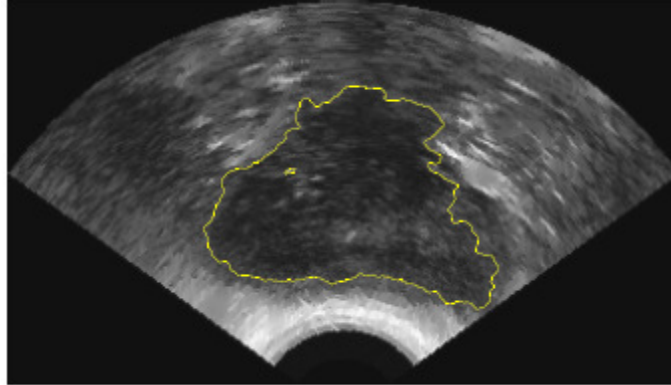


**FIGURE 4:** The deformations of the level set where the contour converges and stops in the vicinity of the prostate boundary.

### 3. Results

As depicted in Fig. 1, TRUS prostate images have very weak contrast, are corrupted with the speckle noise, have short range of gray levels, maintain very weak prostate region texture, and are defected by shadow regions. Although the segmentation of Fig. 1(Top) seems to be less challenging, Fig. 1(Bottom) is very difficult to be segmented. The ordinary image analysis methods perform very poorly for segmentation of prostate region in poor contrast TRUS images.

The proposed extended anisotropic diffusion and its adaptive version are applied for image enhancement and feature extraction. Application of extended anisotropic diffusion in eight directions is depicted in Fig. 2. Fig. 3(b) shows the maximum diffusion obtained over independently computed directional diffusions. As we can observe, independent directional diffused images provide rich features to be used for segmentation and analysis. Deformations of different contours over specific diffusion directions are superimposed on the unprocessed image in Fig. 3(c).

As it is depicted in Fig. 3, not only the contrast is improved, but also some features of prostate region are recovered. Moreover, the directional diffusion features can be effectively used to segment the prostate region. For example, these features can be used in conjunction with structure tensor and vector flow to design the diffusion based velocity functions. The application of adaptive conduction to TRUS image is depicted in Fig. 3(d). The adaptive conduction is computed based on prostate region statistics where mean and standard deviation are computed over the level set contour. A sample segmentation of the TRUS image superimposed on the original image is depicted in Fig. 4.

### 4. Conclusions and Discussions

Prostate texture analysis is a very difficult and challenging task due to the poor contrast, weak texture structure, the speckle noise, and shadow regions. Hence the standard and conventional image processing methods are not capable of segmentation of the prostate region. In this paper we introduced an adaptive anisotropic diffusion method to improve the selective within-region image smoothness while preserving the region boundaries. Moreover, the anisotropic diffusion is extended to eight directions, i.e., four directional pairs such that diffusion in each direction is computed independently yielding a rich feature set for ultrasound image enhancement and analysis. The preliminary results are quite promising, leading to our future work to extend the method to be employed for multiple region segmentation.

## 5. REFERENCES

1. Cancer facts and figures, <http://www.cancer.org>, American Cancer society.
2. C.K. Kwoh, M. Teo, W. Ng, S. Tan, and M. Jones, "Outlining the prostate boundary using the harmonics method", *Med. Biol. Eng. Computing*, 36:768-771, 1998.
3. R.G. Aarnink, R.J.B. Giesen, A. L. Huynen, J. J. de la Rosette, F.M. Debruyne, and H. Wijkstra "A practical clinical method for contour determination in ultrasound prostate images", *Ultrasound Med. Biol.*, 20:705-717, 1994.
4. R.G. Aarnink, S.D. Pathak, J. J. de la Rosette, F.M. Debruyne, Y. Kim, and H. Wijkstra, "Edge detection in ultrasound prostate images using integrated edge map", *Ultrasound Med. Biol.*, 36:635-642, 1998.
5. Y. Zhan and D. Shen, "Deformable segmentation of 3-d ultrasound prostate images using statistical texture matching method", *IEEE Transactions on Medical Imaging*, 25(3):256-272, 2006.
6. D. Freedman, R.J. Radke, T. Zhang, Y. Jeong, D.M. Lovelock, and G.T.Y. Chen, "Model-based segmentation of medical imagery by matching distributions", *IEEE Transactions on Medical Imaging*, 24:281-292, 2005.
7. A. Ghanei, H. Soltanian-Zadeh, A. Ratkewicz, and F. Yin, "A three dimensional deformable Model for segmentation of human prostate from ultrasound images", *Med. Phys*, 28:2147-2153, 2001.
8. C. Knoll, M. Alcaniz, V. Grau, C. Monserrat, and M. Juan, "Outlining of the prostate using snakes with shape restrictions based on the wavelet transform", *Pattern Recognition*, 32:1767-1781, 1999.
9. S. D. Pathak, V. Chalana, D. haynor, and Y. kim, "Edge guided boundary delineation in prostate ultrasound images", *IEEE Transactions on Medical Imaging*, 19:1211-1219, 2000.
10. S. S. Mohamed, T. K. Abdel-galil, M. M. Salma, A. Fenster, D. B. Downey, and K. Rizkalla, "Prostate cancer diagnosis based on gabor filter texture segmentation of ultrasound image", *IEEE CCECE*, 1485-1488, 2003.
11. P. Perona and J. Malik, "Scale-space and edge detection using anisotropic diffusion", *IEEE Trans. on Pattern Analysis and Machine Intelligence*, 12(7):629-639, 1990.
12. G. Gerig, O. Kbler, R. Kikinis, , and F. Jolesz, "Nonlinear anisotropic filtering of MRI data", *IEEE Transactions on Medical Imaging*, 11(2):221-232, 1992.
13. G. Sapiro and A. Tannenbaum, "Edge preserving geometric smoothing of MRI data", Technical report, University of Minnesota, Dept. of Electrical Engineering, 1994.